IEEE Photonics Journal
An IEEE Photonics Society Publication

Open Access

IEEE 802.15.3c WPAN Standard Using Millimeter Optical Soliton Pulse Generated by a Panda Ring Resonator

Volume 5, Number 5, October 2013

I. S. Amiri
S. E. Alavi
Sevia M. Idrus
A. Nikoukar
J. Ali

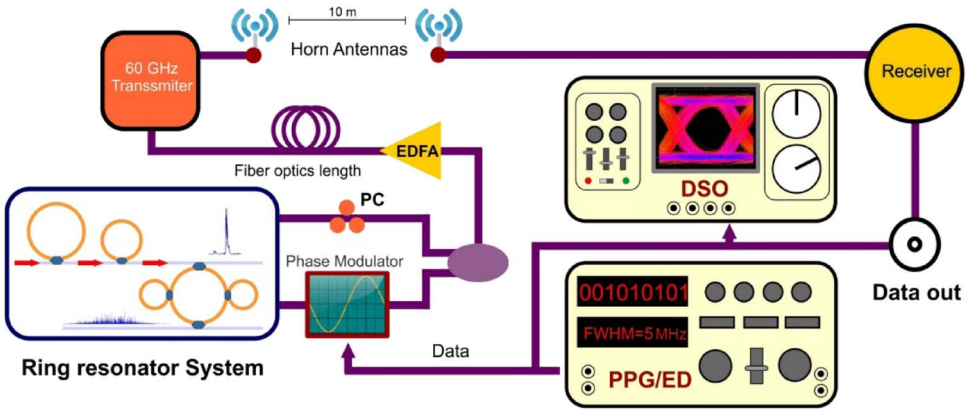

DOI: 10.1109/JPHOT.2013.2280341
1943-0655 © 2013 IEEE

IEEE photonics SOCIETY

IEEE

IEEE 802.15.3c WPAN Standard Using Millimeter Optical Soliton Pulse Generated by a Panda Ring Resonator

I. S. Amiri,[1] S. E. Alavi,[2] Sevia M. Idrus,[2] A. Nikoukar,[3] and J. Ali[1]

[1]Institute of Advanced Photonics Science, Nanotechnology Research Alliance, Universiti Teknologi Malaysia (UTM), 81310 Johor Bahru, Malaysia
[2]Photonics Lightwave Communication Research Group, Faculty of Electrical Engineering, Universiti Teknologi Malaysia, 81310 Johor Bahru, Malaysia
[3]Faculty of Computing, Universiti Teknologi Malaysia (UTM), 81310 Johor Bahru, Malaysia

DOI: 10.1109/JPHOT.2013.2280341

Manuscript received August 16, 2013; accepted August 20, 2013. Date of publication August 30, 2013; date of current version September 10, 2013. The authors acknowledge the administration of the Universiti Teknologi Malaysia (UTM) and the Research Management Centre (RMC) of UTM for financial support through Geran Universiti Penyelidikan (GUP) funding vote number 04H35. Corresponding author: I. S. Amiri (e-mail: isafiz@yahoo.com).

Abstract: A system of microring resonators (MRRs) connected to an optical modified add/drop filter system known as a Panda ring resonator is presented. The optical soliton pulse of 60 GHz frequency band can be generated and used for Wireless Personal Area Network (WPAN) applications such as IEEE 802.15.3c. The system uses chaotic signals generated by a Gaussian laser pulse propagating within a nonlinear MRRs system. The chaotic signals can be generated via a series of microring resonators, where the filtering process is performed via the Panda ring resonator system wherein ultrashort single and multiple optical soliton pulses of 60 GHz are generated and seen at the through and drop ports, respectively. The IEEE 802.15.3c standard operates at the 60 GHz frequency band, and it is applicable for a short distance optical communication such as indoor systems, where the higher transmission data rate can be performed using a high frequency band of the output optical soliton pulses. The single and multi-soliton pulses could be generated and converted to logic codes, where the bandwidths of these pulses are 5 and 20 MHz, respectively. Thus, these types of signals can be used in optical indoor systems and transmission link using appropriate components such as transmitter, fiber optics, amplifier, and receiver.

Index Terms: Optical soliton pulses, Wireless Personal Area Network, 60 GHz frequency band.

1. Introduction

In 2001, the Federal Communications Commission (FCC) allocated the 57–64 GHz band for unlicensed use [1], [2]. Unlicensed frequencies, such as 2.4 GHz band and, perhaps, 5 GHz band, in near future, will become more and more crowded; therefore, the new networking wireless technology has to move to other spectrum areas in which very high bit-rate connectivity can be provided [3]–[5]. The 60 GHz frequency band is very promising, since it offers a huge amount of unlicensed spectrum that provides very high throughput [6]. Some standardization groups and industrial consortia have been formed to specify 60 GHz transmission for Wireless Personal Area Network (WPAN) applications, where the main initiatives are IEEE 802.15.3c [7]. The standard focuses on the indoor over Gb/s data rate wireless communication and operates at the 60 GHz frequency band [8], [9]. This

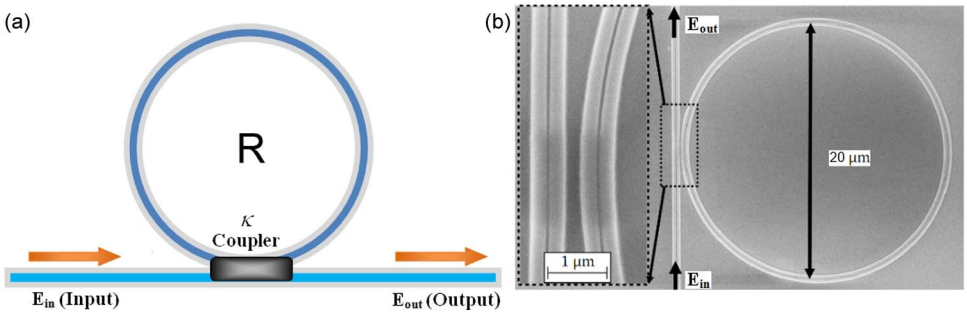

Fig. 1. (a) A nonlinear microring resonator. (b) Scanning electron micrograph of a microring resonator with a radius of 20 μm,R: ring's radius, κ: coupling coefficient, E_{in}: input power, E_{out}: output power.

standard shows that the system supports both single carrier and OFDM transmission [10], [11]. A WPAN system is considered to supply short-range and very-high-speed multimedia data services to computer terminals and consumer appliances, which can be located in rooms, office spaces, "hot spots," and kiosks [12].

Compared to Wireless Local Area Networks (WLANs), such as the popular 802.11a/b/g "WiFi" systems, WPANs can be used to provide higher data rates, but shorter range [13], [14]. Researchers have found many concerns on the high bandwidth available in the 60 GHz unlicensed spectrum band [15], [16]. This is due to the potential to attain wireless communication speeds in excess of 1 Gb/s, appropriate for the transmission of uncompressed, high-definition TV (HDTV), music, and high resolution images [17], [18]. IEEE 802.I5.3c intends to standardize the physical (PHY) and medium access control (MAC) operation of 60 GHz WPANs [19].

An optical ring resonator is a set of wavelengths in which at least one is a closed loop coupled with some sort of light input and output. The ring resonators use light and obey the properties behind constructive interference and total internal reflection. When the light of the resonant wavelength is passed through the loop from the input port, it builds up in intensity over multiple round-trips due to constructive interference and is output to the output port, which serves as a detector waveguide. The optical ring resonator functions as a filter because only a select few wavelengths will be at resonance within the loop. The ring resonator can be integrated with two or more ring waveguides to form an add-drop filter system or a Panda ring resonator system [20], [21]. A microring resonator [22] can be used to generate a broad band of optical soliton applicable in many areas of optical networks such as wireless-cable systems and indoor-outdoor communication [23], [24]. The simulation and scanning electron micrograph of a microring resonator with a radius of 20 μm is shown in Fig. 1.

Amiri *et al.* have reported the optical output transfer function that is derived and used for a light pulse propagating within a microring resonator at a resonant condition [25]. The broad spectrum of light pulse can be transformed to the discrete pulses after filtering [26]. Using the optical soliton pulses, the optical bandwidth can be enlarged or compressed within the nonlinear microring resonator [27]. The superposition of self-phase and cross-phase soliton pulse modulation [28] within a nanowaveguide can be observed, whereas large output signals can be obtained [29]. The optimum energy of the soliton can be coupled into the waveguide by a larger effective core area of the ring resonator [30].

Suitable coupling power is required in order to maintain the soliton pulse propagating within the system [31]. Here, the interference signal is a minor effect compared to the loss associated with the direct passing through [32]. The frequency band generation can be obtained via the system, whereas enlargement of the capacity of communication channels is performed [33]. The long distance communication can be performed by using high optical output of the soliton signals within the ring resonator system. Powerful light can be obtained by using a high-power light source or a ring resonator with a smaller radius [34], [35]. A soliton band can be generated by using a Gaussian laser pulse propagating within a ring resonator system [36].

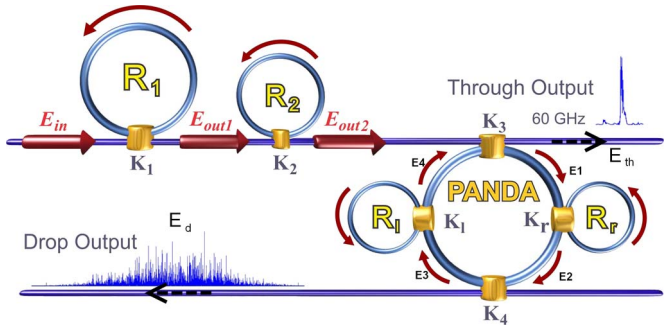

Fig. 2. Schematic diagram of a Panda ring resonator system connected to two ring resonators, where R: ring's radius, κ: coupling coefficient, E_{in}: input power.

We use a system of microring resonators connecting to a modified add/drop system known as a Panda ring resonator system to generate a high frequency band of optical soliton pulses. Here, the multifunction operations of the Panda ring resonator system are employed in order to control, tune, and amplify the output signals, whereas the Gaussian laser pulse can be introduced into the system.

2. Theoretical Background

The system known as a Panda ring resonator is connected to a series of ring resonators R_1 and R_2, as shown in Fig. 2. The input signal can be inserted into the system via the input port. Here, a mathematical equation of the propagating input pulse inside the nonlinear ring system has been solved in order to show the nonlinear behavior of the output signals.

The Kerr effect is a change in the refractive index of a material in response to an applied electric field. The optical Kerr effect or the AC Kerr effect is the case in which the electric field is due to the light itself. This causes a variation in index of refraction, which is proportional to the local irradiance of the light. This refractive index variation is responsible for the nonlinear optical effects of self-focusing and self-phase modulation (SPM). This effect only becomes significant with very intense beams such as those from lasers [37], [38]. Therefore, the Kerr effect causes the refractive index (n) of the medium to vary, where it is given by [39]

$$n = n_0 + n_2 I = n_0 + P \times n_2 / A_{\text{eff}} \tag{1}$$

with n_0 and n_2 as the linear and nonlinear refractive indexes, respectively [40]. I and P are the optical intensity and the power, respectively [41]. The effective mode core area of the device is given by A_{eff}. For a ring resonator design, A_{eff} ranges from 0.50 to 0.10 μm^2, regarding to practical material parameters (InGaAsP/InP). A pulse with a temporal intensity profile that has a Gaussian shape is defined as a Gaussian laser pulse. The Gaussian laser pulse with a central wavelength of 50 GHz and power of 2.8 W is introduced into the first ring resonator R_1, where it is expressed by E_{in}. The input optical field of the Gaussian laser pulse is given by

$$E_{in}(t) = E_0 \exp\left[\left(\frac{z}{2L_D}\right) - i\omega_0 t\right] \tag{2}$$

E_0 and z are the amplitude of the optical field and the propagation distance, respectively. L_D is the dispersion length of the soliton pulse [42], where the carrier frequency of the signal is ω_0. The Gaussian laser pulse propagates as soliton pulses; thus, it keeps its temporal width invariance while it propagates, and therefore, it is called a temporal soliton. A balance should be achieved between the dispersion length (L_D) and the nonlinear length $(L_{\text{NL}} = 1/\Gamma\phi_{\text{NL}})$. Here, $\Gamma = n_2 \times \kappa_0$, is the length scale over which disperse or nonlinear effects make the beam become wider or narrower; hence, $L_D = L_{\text{NL}}$ [43]. The normalized output of the light field, which is the

ratio between the output and input fields $E_{out}(t)$ and $E_{in}(t)$ for two ring resonators, can be expressed by

$$\left|\frac{E_{out1}(t)}{E_{in}(t)}\right|^2 = (1-\gamma_1)\left[1 - \frac{\left(1-(1-\gamma_1)x_1^2\right)\kappa_1}{\left(1-x_1\sqrt{1-\gamma_1}\sqrt{1-\kappa_1}\right)^2 + 4x_1\sqrt{1-\gamma_1}\sqrt{1-\kappa_1}\sin^2\left(\frac{\phi_1}{2}\right)}\right] \tag{3}$$

$$\left|\frac{E_{out2}(t)}{E_{out1}(t)}\right|^2 = (1-\gamma_2)\left[1 - \frac{\left(1-(1-\gamma_2)x_2^2\right)\kappa_2}{\left(1-x_2\sqrt{1-\gamma_2}\sqrt{1-\kappa_2}\right)^2 + 4x_2\sqrt{1-\gamma_2}\sqrt{1-\kappa_2}\sin^2\left(\frac{\phi_2}{2}\right)}\right]. \tag{4}$$

κ and γ are the coupling coefficient and the fractional coupler intensity loss, respectively; $x = \exp(-\alpha L/2)$ represents a round-trip loss coefficient, where the waveguide length and the linear absorption coefficient are given by L and α, respectively. Here, $\phi = \phi_0 + \varphi_{\mathrm{NL}}$, where $\phi_0 = k_n L n_0$ and $\phi_{\mathrm{NL}} = k_n L n_2 |E_{in}|^2$ are the linear and nonlinear phase shifts. The wave propagation number in a vacuum is given by $k_n = 2\pi/\lambda$, where λ is the input wavelength light field. For the Panda ring resonator system, the output signals inside the system are given as follows [44]:

$$E_1 = \sqrt{1-\gamma_3}\left(\sqrt{1-\kappa_3}E_4 + j\sqrt{\kappa_3}E_{out2}\right) \tag{5}$$

$$E_2 = E_r E_1 e^{-\frac{\alpha LP}{2\,2} - jk_n\frac{LP}{2}}. \tag{6}$$

Here, $LP = 2\pi R_{Panda}$, where R_{Panda} is the radius of the Panda ring resonator system. The electric field of the right ring of the Panda ring resonator system is given by [45], [46]

$$E_r = E_1 \frac{\sqrt{(1-\gamma_r)(1-\kappa_r)} - (1-\gamma_r)e^{-\frac{\alpha}{2}L_r - jk_n L_r}}{1 - \sqrt{1-\gamma_r}\sqrt{1-\kappa_r}e^{-\frac{\alpha}{2}L_r - jk_n L_r}}. \tag{7}$$

Inserting equation (7) into equation (6) results as

$$E_2 = \sqrt{1-\gamma_r}\left(\sqrt{1-\kappa_r}E_1 + j\sqrt{\kappa_r}E_{r2}\right) \tag{8}$$

where

$$E_{r2} = E_{r1}e^{-\frac{\alpha}{2}L_r - jk_n L_r} \tag{9}$$

$$E_{r1} = \sqrt{1-\gamma_r}\left(\sqrt{1-\kappa_r}E_{r2} + j\sqrt{\kappa_r}E_1\right). \tag{10}$$

E_{r1} and E_{r2} are the round-trip light fields of the right ring and are given by

$$E_{r1} = \frac{j\sqrt{1-\gamma_r}\sqrt{\kappa_r}E_1}{1 - \sqrt{1-\gamma_r}\sqrt{1-\kappa_r}e^{-\frac{\alpha}{2}L_r - jk_n L_r}} \tag{11}$$

$$E_{r2} = \frac{j\sqrt{1-\gamma_r}\sqrt{\kappa_r}E_1 e^{-\frac{\alpha}{2}L_r - jk_n L_r}}{1 - \sqrt{1-\gamma_r}\sqrt{1-\kappa_r}e^{-\frac{\alpha}{2}L_r - jk_n L_r}}. \tag{12}$$

$L_r = 2\pi R_r$, where R_r is the radius of the right ring. Light fields on the left side of the Panda ring resonator system can be expressed as

$$E_3 = \sqrt{1-\gamma_4} \times \sqrt{1-\kappa_4}E_2 \tag{13}$$

$$E_4 = E_l E_3 e^{-\frac{\alpha LP}{2\,2} - jk_n\frac{LP}{2}} \tag{14}$$

where

$$E_l = E_3 \frac{\sqrt{(1-\gamma_l)(1-\kappa_l)} - (1-\gamma_l)e^{-\frac{\alpha}{2}L_l - jk_n L_l}}{1 - \sqrt{1-\gamma_l}\sqrt{1-\kappa_l}e^{-\frac{\alpha}{2}L_l - jk_n L_l}}. \tag{15}$$

TABLE 1

Parameters of the microring resonator system

Fixed Parameters:	Value
R_1 = First ring's radius of the system	5 μm
R_2 = Second ring's radius of the system	3 μm
R_r = Right ring's radius of the Panda ring resonator system	1 μm
R_l = Left ring's radius of the Panda ring resonator system	1 μm
R_{Panda} = Centered ring's radius of the Panda ring resonator system	100 μm
κ_1 = Coupling coefficient of the ring (R_1)	0.5
κ_2 = Coupling coefficient of the ring (R_2)	0.3
κ_3 = Coupling coefficient of the ring (R_{Panda})	0.17
κ_4 = Coupling coefficient of the ring (R_{Panda})	0.05
κ_r = Coupling coefficient of the ring (R_r)	0.02
κ_l = Coupling coefficient of the ring (R_l)	0.02
n_0 = Linear refractive index	3.34
γ = Fractional coupler intensity loss	0.01
n_2 = Nonlinear refractive index	$2.2\times10^{-17} m^2 W^{-1}$
α = Ring resonator loss	0.5 $dBmm^{-1}$
A_{eff1} = Effective core area of the ring (R_1)	0.25 μm^2
A_{eff2} = Effective core area of the ring (R_2)	0.10 μm^2
A_{effr} = Effective core area of the ring (R_r)	0.10 μm^2
A_{effl} = Effective core area of the ring (R_l)	0.10 μm^2
E_{in} = Input power at input port	2.8 W
λ_0 = Central wavelength	50 GHz

Here, $L_l = 2\pi R_l$, and R_l is the radius of the left ring. Therefore, the output signals from the through and drop ports of the Panda ring resonator system can be expressed as

$$E_{th} = \sqrt{1-\gamma_3}\left[\sqrt{1-\kappa_3}E_{out2} + j\sqrt{\kappa_3}E_4\right] \tag{16}$$

$$E_d = \sqrt{1-\gamma_4} \times j\sqrt{\kappa_4}E_2. \tag{17}$$

In order to simplify these equations, the parameters of x_a, x_b, y_a, and y_b are defined as

$$x_a = (1-\gamma_3)^{\frac{1}{2}}, x_b = (1-\gamma_4)^{\frac{1}{2}}, y_a = (1-\kappa_3)^{\frac{1}{2}}, \text{and } y_b = (1-\kappa_4)^{\frac{1}{2}}.$$

Therefore

$$E_1 = \frac{jx_a\sqrt{\kappa_3}E_{out2}}{1 - x_a x_b y_a y_b E_r E_l e^{-\frac{\alpha}{2}LP - jk_n LP}} \tag{18}$$

$$E_2 = \frac{E_r \times jx_a\sqrt{\kappa_3}E_{out2} \times e^{-\frac{\alpha LP}{2\,2} - jk_n\frac{LP}{2}}}{1 - x_a x_b y_a y_b E_r E_l e^{-\frac{\alpha}{2}LP - jk_n LP}} \tag{19}$$

$$E_3 = x_b y_b E_r E_1 e^{-\frac{\alpha LP}{2\,2} - jk_n\frac{LP}{2}} \tag{20}$$

$$E_4 = x_b y_b E_r E_l E_1 e^{-\frac{\alpha}{2}LP - jk_n LP} \tag{21}$$

$$E_{th} = x_a(y_a E_{out2} + j\sqrt{\kappa_3}E_4) \tag{22}$$

$$E_d = x_b \times j\sqrt{\kappa_4}E_2. \tag{23}$$

Results based on the nonlinear equations of the ring resonators can be obtained where the parameters of the system affect the output signals significantly.

3. Results and Discussion

The millimeter wavelength input pulse of a Gaussian laser pulse with power of 2.8 W is inserted into the system. The parameters of the system are presented in Table 1.

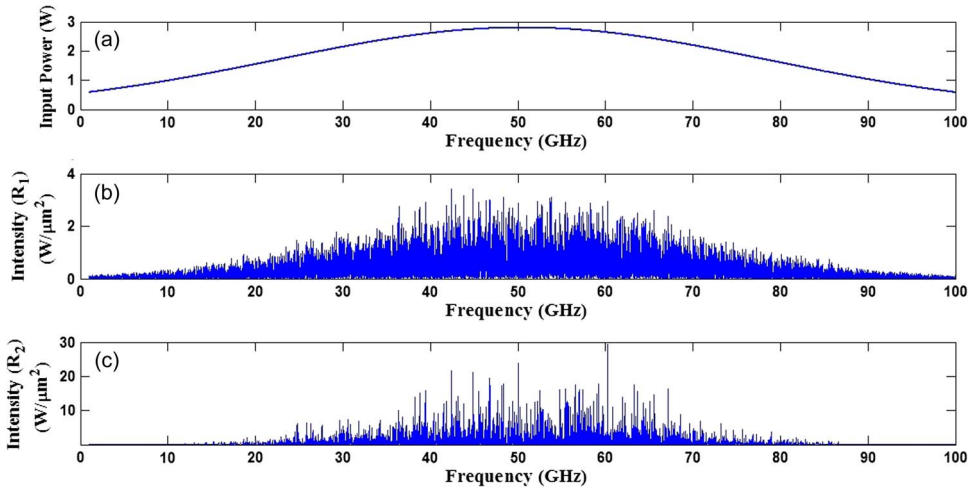

Fig. 3. Chaotic signal generation, where (a) input power, (b) output chaotic signals from R_1, and (c) output chaotic signals from R_2.

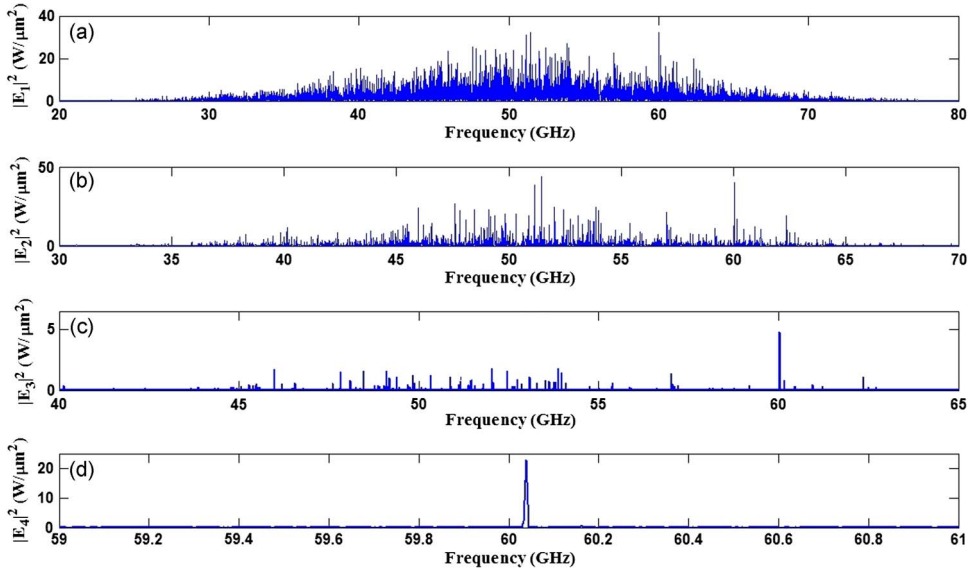

Fig. 4. Interior soliton signals, where (a) $|E_1|^2$ (W), (b) $|E_2|^2$ (W/μm^2), (c) $|E_3|^2$ (W/μm^2), and (d) $|E_4|^2$ (W/μm^2).

The results of the chaotic signal generation are shown in Fig. 3. A large bandwidth within the microring device can be generated by propagating a Gaussian laser pulse input into the nonlinear MRRs, where the required signals perform the secure communication network.

The signal is chopped (sliced) into a smaller signal spreading over the spectrum, which shows that the large bandwidth is formed within the first ring device. The compress bandwidth is obtained within the ring R_2. A frequency soliton pulse can be formed and trapped within the Panda ring resonator system with suitable ring parameters. Interior soliton signals inside the Panda ring resonator system can be seen in Fig. 4, where the filtering and trapping process occurs during the propagation of the input Gaussian laser beam inside the centered ring of the Panda ring resonator system. The chaotic pulses are used widely in secured optical communication as carrier signals in which the information is input into the signals and, finally, can be retrieved by using suitable filtering

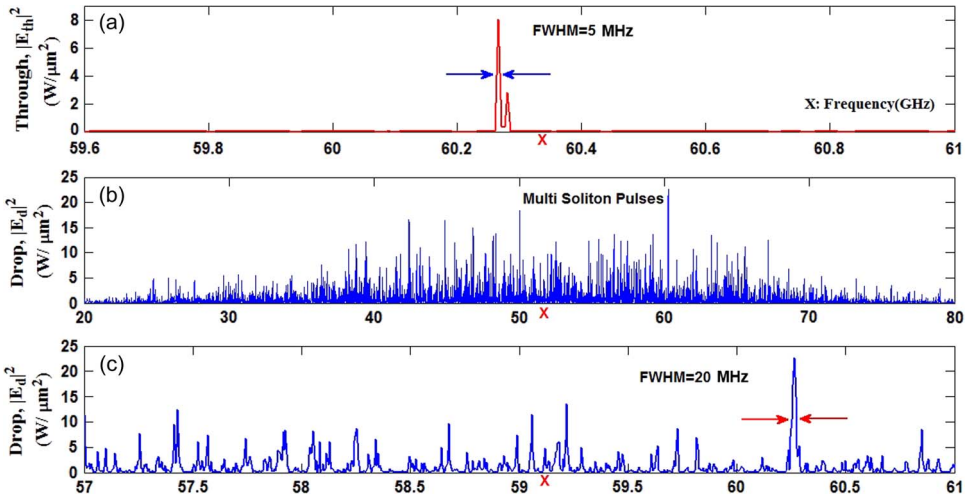

Fig. 5. Results of single and multifrequency soliton trapping, where (a) throughput output signal (single soliton pulse with FWHM = 5 MHz), (b) multi-soliton pulses, and (c) multi-soliton pulses ranges from 57 to 61 GHz with FWHM = 20 MHz.

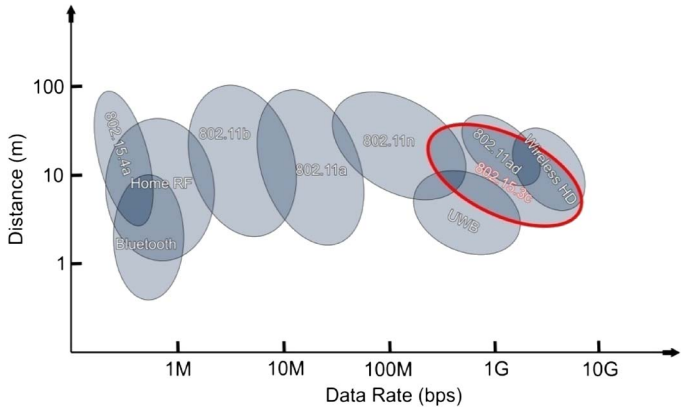

Fig. 6. Data rate versus the distance for WLAN and WPAN standards [50].

systems. Fig. 4(a) and (b) shows the interior generated signals on the right side of the Panda ring resonator system, where Fig. 4(c) and (d) shows the power of the left side.

Filtering of the interior soliton signals can be performed when generated pulses pass through the couplers, i.e., κ_3 and κ_4. The output signals from the throughput and drop ports of the system can be seen in Fig. 5, where single and multi-soliton ranges from 57 to 61 GHz are generated and used in many optical communication WPAN applications such as IEEE 802.15.3c.

The bit rate transmission of the IEEE 802.15.3c can be seen in Fig. 6. The millimeter-wave WPAN permits very high data rate above 2 Gbit/s applications such as high speed Internet access, streaming content download, real time streaming, and wireless data bus for cable replacement [47], [48]. Therefore, optional data rates in excess of 3 Gbit/s will be provided [49].

Generated optical soliton pulses with an optical frequency range of 60 GHz can be propagated via a network indoor system shown in Fig. 7, where the multi-soliton pulses can be used in order to increase the capacity of the optical system.

The transmission of the single and multi-soliton pulses can be obtained by converting the signals into the logic codes as shown in Fig. 8. The threshold intensity power has been selected

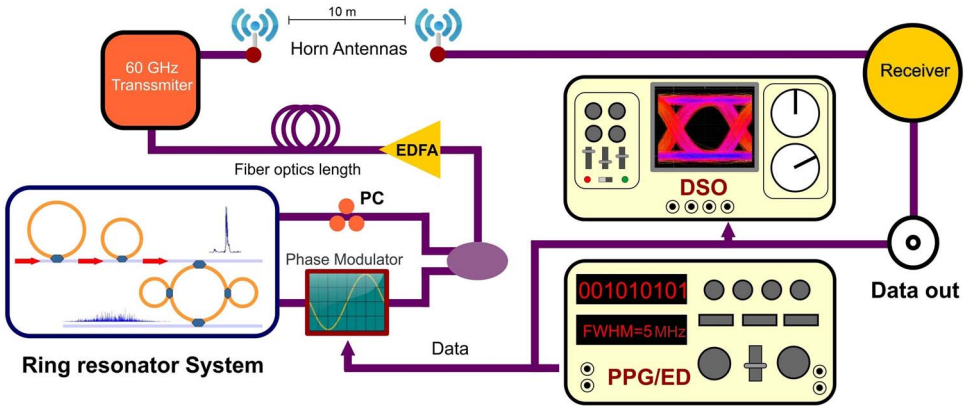

Fig. 7. Schematic of optical signal transmission link for 60 GHz soliton pulses. PC: polarization controller, EDFA: erbium doped fiber amplifier, PPG/ED: pulse-pattern generator/error detector, and DSO: digital storage oscilloscope.

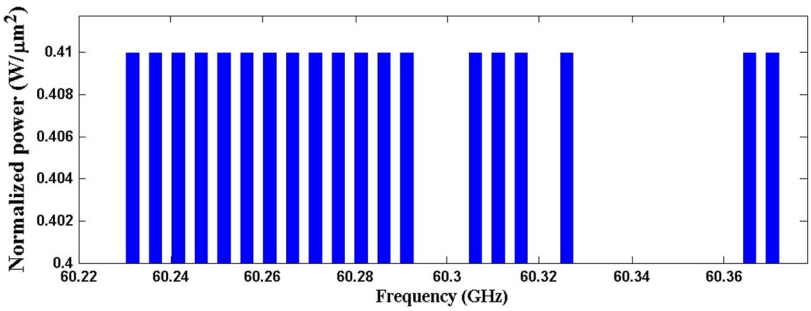

Fig. 8. Generation of logic codes of "0" and "1," where the generated logic code is "00111111111111100111010000000110".

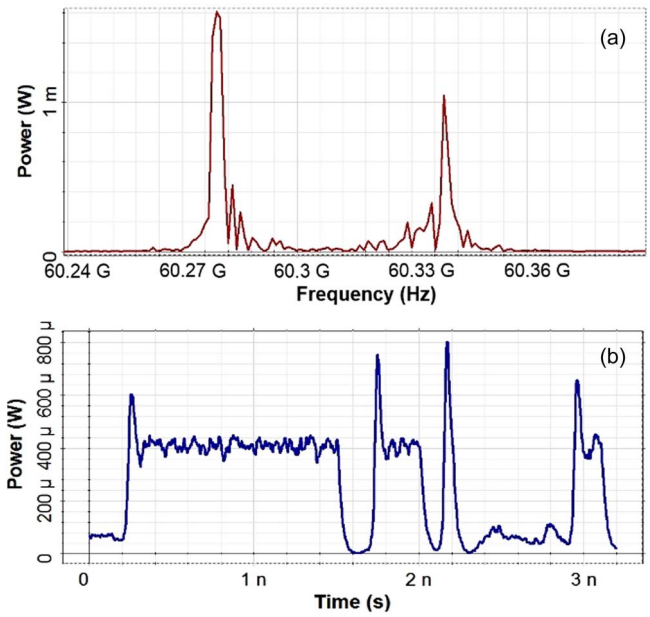

Fig. 9. Transmission of soliton logic codes along the fiber optics with length of 1 km, where (a) single soliton pulses within ranges from 60.24 to 60.39 GHz, (b) multi-soliton within the range of 60.22–60.38 GHz.

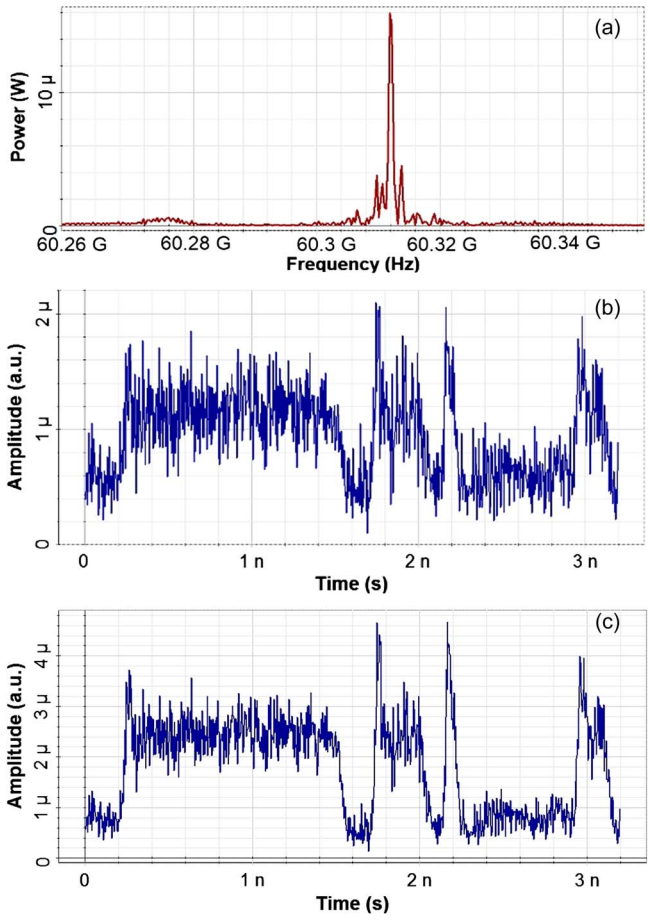

Fig. 10. Transmission of single and multi-soliton pulses using an optical wireless transmitter within a 10 m range, where (a) single soliton pulse at 60.31 GHz, (b) multi-soliton within the range of 60.22–60.38 GHz, and (c) filtered and amplified multi-signal.

to 0.40–0.41 W/μm^2. For the multi-soliton pulses, the frequency range has been selected to 60.22–60.38 GHz, where the generated logic code is "00111111111111100111010000000110".

Therefore, the multiple optical soliton can be converted to logic codes using a suitable analog to digital converter. The transmission of the logic codes can be performed within a wired/wireless network, where the high capacity of transmission can be implemented by using multi-soliton pulses. In Fig. 7, the fiber optic has a length of 1 km, attenuation of 0.2 dB/km, dispersion of 5 ps/nm/km, the differential group delay of 0.2 ps/km, the nonlinear refractive index of 2.6×10^{-20} m^2/W, the effective area of 25 μm^2, and the nonlinear phase shift of 3 mrad. The transmitted signals of single and multi-soliton pulses in the form of logic codes along the fiber optics are shown in Fig. 9.

The advanced transmitter topologies are desirable for application in both mobile and fixed wireless telecommunication inasmuch as they are able to provide power-efficient amplification of signals with large peak-to-average power ratios (PAPRs) without compromising system linearity. The optical wireless transmitter has an extinction ration of 10 dB; a line width of 10 THz, modulation type of nonreturn-to-zero (NRZ); and a rise time of 1/(bit rate) $\times$ 0.05, where the optical receiver has responsivity of 1 A/W; a dark current of 10 nA, a cutoff frequency of 0.75*bit rate Hz; and a thermal noise of 10^{-22} W/Hz. The transmission of soliton signals (see Fig. 9), using the wireless transmitter, is shown in Fig. 10, where the covering range is 10 m.

Fig. 11 shows the bit error rate (BER) performance of the used system under an indoor AWGN channel. As it can be observed from this figure, the BER for received power of 5 μW is around 10^{-3}, which is not suitable for indoor communication applications. Therefore, for the received power

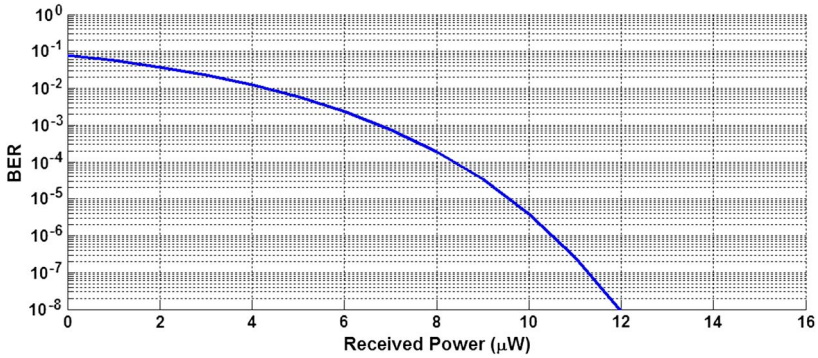

Fig. 11. Bit Error Rate (BER) Versus the Received Power (μW).

above 5 μW, the BER decreases, which shows high performance of the optical indoor communication systems.

The advantage of the ring resonator system is that controlling of the optical parameters, such as the output power, signal bandwidth, frequency band range, free spectrum range, and FWHM, is plausible. Therefore, transmission of signals can be performed via an indoor optical communication link. For the outdoor applications, powerful output soliton pulses are required, where the capacity of the system can be performed by using multiple optical soliton pulses.

4. Conclusion

A system of microring resonators for WPAN indoor optical communication has been demonstrated. The optical soliton is generated by the Gaussian laser pulse propagating within a microring resonator system connected to a Panda ring resonator system. A high-frequency band of optical soliton pulses can be used in optical communication networks such as WPAN and IEEE 802.15.3c indoor systems, in which very high bit-rate connectivity can be provided. The loss of the transmission system can be compensated by using multiple optical soliton frequency band ranges 57–61 GHz, where the receiver is provided at the end of the transmission link. Here, a single soliton pulse with an FWHM of 5 MHz is generated, where the multi-soliton pulses have an FWHM of 20 MHz. These pulses can be transmitted along the wired/wireless transmission link. Therefore, the WPAN indoor system, which presents short distance optical communication, can be performed by using the generated GHz band frequency optical soliton pulses.

Acknowledgment

I. S. Amiri would like to thank the Institute of Advanced Photonics Science, Nanotechnology Research Alliance, and Universiti Teknologi Malaysia (UTM).

References

[1] N. Guo, R. C. Qiu, S. S. Mo, and K. Takahashi, "60-GHz millimeter-wave radio: Principle, technology, and new results," *EURASIP J. Wireless Commun. Netw.*, vol. 2007, p. 48, Dec. 2007.
[2] D. J. Chung, A. L. Amadjikpè, and J. Papapolymrou, "3D integration of a band selective filter and antenna for 60 GHz applications," in *Proc. IEEE Antennas Propag. Soc. Int. Symp.*, 2010, pp. 1–4.
[3] G. R. Aiello and G. D. Rogerson, "Ultra-wideband wireless systems," *IEEE Microw. Mag.*, vol. 4, no. 2, pp. 36–47, Jun. 2003.
[4] J. M. Gilbert, C. H. Doan, S. Emami, and C. B. Shung, "A 4-Gbps uncompressed wireless HD A/V transceiver chipset," *IEEE Micro*, vol. 28, no. 2, pp. 56–64, Mar./Apr. 2008.
[5] X. Pang, A. Caballero, A. Dogadaev, V. Arlunno, L. Deng, R. Borkowski, J. S. Pedersen, D. Zibar, X. Yu, and I. T. Monroy, "25 Gbit/s QPSK hybrid fiber-wireless transmission in the W-band (75–110 GHz) with remote antenna unit for in-building wireless networks," *IEEE Photon. J.*, vol. 4, no. 3, pp. 691–698, Jun. 2012.
[6] C. Park and T. S. Rappaport, "Short-range wireless communications for next-generation networks: UWB, 60 GHz millimeter-wave WPAN, and ZigBee," *IEEE Wireless Commun.*, vol. 14, no. 4, pp. 70–78, Aug. 2007.

[7] M. Lei, I. Lakkis, H. Harada, and S. Kato, "MMSE-FDE based on estimated SNR for single-carrier block transmission (SCBT) in multi-Gbps WPAN (IEEE 802.15. 3c)," in *Proc. IEEE Int. Conf. Commun. Workshops*, 2008, pp. 52–56.
[8] R. C. Daniels and R. W. Heath, "60 GHz wireless communications: Emerging requirements and design recommendations," *IEEE Veh. Technol. Mag.*, vol. 2, no. 3, pp. 41–50, Sep. 2007.
[9] P. Li, H. Chen, M. Chen, and S. Xie, "Gigabit/s photonic generation, modulation, and transmission for a reconfigurable impulse radio UWB over fiber system," *IEEE Photon. J.*, vol. 4, no. 3, pp. 805–816, Jun. 2012.
[10] M. Kuschnerov, M. Chouayakh, K. Piyawanno, B. Spinnler, E. de Man, P. Kainzmaier, M. S. Alfiad, A. Napoli, and B. Lankl, "Data-aided versus blind single-carrier coherent receivers," *IEEE Photon. J.*, vol. 2, no. 3, pp. 387–403, Jun. 2010.
[11] E. Giacoumidis, J. Wei, X. Yang, A. Tsokanos, and J. Tang, "Adaptive-modulation-enabled WDM impairment reduction in multichannel optical OFDM transmission systems for next-generation PONs," *IEEE Photon. J.*, vol. 2, no. 2, pp. 130–140, Apr. 2010.
[12] R. Fisher, "60 GHz WPAN standardization within IEEE 802.15. 3c," in *Proc. Int. Symp. Signals, Syst. Electron.*, 2007, pp. 103–105.
[13] J. Karaoguz, "High-rate wireless personal area networks," *IEEE Commun. Mag.*, vol. 39, no. 12, pp. 96–102, Dec. 2001.
[14] A. Soomro and D. Cavalcanti, "Opportunities and challenges in using WPAN and WLAN technologies in medical environments [Accepted from Open Call]," *IEEE Commun. Mag.*, vol. 45, no. 2, pp. 114–122, Feb. 2007.
[15] C. H. Doan, S. Emami, D. Sobel, A. M. Niknejad, and R. W. Brodersen, "60 GHz CMOS radio for Gb/s wireless LAN," in *Proc. IEEE Radio Freq. Integr. Circuits Symp. Dig. Papers*, 2004, pp. 225–228.
[16] P. Smulders, "Exploiting the 60 GHz band for local wireless multimedia access: Prospects and future directions," *IEEE Commun. Mag.*, vol. 40, no. 1, pp. 140–147, Jan. 2002.
[17] J. Walrand and P. P. Varaiya, *High-Performance Communication Networks*. San Mateo, CA, USA: Morgan Kaufmann, 2000.
[18] Y. Tashiro, Y. Yashima, and H. Fuju, "NTT's technologies for next-generation video services," *CIE, Theor. Pract. Comput.*, vol. 4, no. 1, p. 9, Jan. 2006.
[19] S. Singh, F. Ziliotto, U. Madhow, E. M. Belding, and M. J. W. Rodwell, "Millimeter wave WPAN: Cross-layer modeling and multi-hop architecture," in *Proc. IEEE Int. Conf. Comput. Commun.*, 2007, pp. 2336–2340.
[20] J. Dong, L. Liu, D. Gao, Y. Yu, A. Zheng, T. Yang, and X. Zhang, "Compact notch microwave photonic filters using on-chip integrated microring resonators," *IEEE Photon. J.*, vol. 5, no. 2, p. 5500307, Apr. 2013.
[21] W. Bogaerts, P. De Heyn, T. Van Vaerenbergh, K. De Vos, S. Kumar Selvaraja, T. Claes, P. Dumon, P. Bienstman, D. Van Thourhout, and R. Baets, "Silicon microring resonators," *Laser Photon. Rev.*, vol. 6, no. 1, pp. 47–73, Jan. 2012.
[22] I. S. Amiri, R. Ahsan, A. Shahidinejad, J. Ali, and P. P. Yupapin, "Characterisation of bifurcation and chaos in silicon microring resonator," *IET Commun.*, vol. 6, no. 16, pp. 2671–2675, Nov. 2012.
[23] E. Ekmekci, K. Topalli, T. Akin, and G. Turhan-Sayan, "A tunable multi-band metamaterial design using micro-split SRR structures," *Opt. Exp.*, vol. 17, no. 18, pp. 16 046–16 058, Aug. 2009.
[24] Z. Wu, Y. Ming, F. Xu, and Y. Lu, "Optical frequency comb generation through quasi-phase matched quadratic frequency conversion in a micro-ring resonator," *Opt. Exp.*, vol. 20, no. 15, pp. 17 192–17 200, Jul. 2012.
[25] I. S. Amiri, A. Afroozeh, M. Bahadoran, J. Ali, and P. P. Yupapin, "Molecular transporter system for Qubits generation," *J. Teknol.*, vol. 55, no. S1, pp. 155–165, May 2011.
[26] U. Dunmeekaew, N. Pornsuwancharoen, and P. Yupapin, "New wavelength division multiplexing bands generated by using a Gaussian pulse in a microring resonator system," *Microw. Opt. Technol. Lett.*, vol. 52, no. 1, pp. 98–101, Jan. 2010.
[27] P. Chamorro-Posada, F. J. Fraile-Pelaez, and F. J. Diaz-Otero, "Micro-ring chains with high-order resonances," *J. LightwaveTechnol.*, vol. 29, no. 10, pp. 1514–1521, May 2011.
[28] Y. V. Bludov, V. V. Konotop, and M. Salerno, "Linear superpositions of gap solitons in periodic Kerr media," *Opt. Lett.*, vol. 36, no. 15, pp. 2856–2858, Aug. 2011.
[29] A. Afroozeh, I. S. Amiri, M. Kouhnavard, M. Jalil, J. Ali, and P. Yupapin, "Optical dark and bright soliton generation and amplification," in *Proc. ESciNano Conf.*, Kuala Lumpur, Malaysia, 2010, pp. 1–3.
[30] M. J. O'Mahony, D. Klonidis, C. Politi, R. Negabati, and D. Simeonidou, "Optical packet switch architectures for ultrahigh-speed networks," in *Proc. SPIE, Opt. Transmiss., Switching Subsyst. III*, vol. 6021, Dec. 8, 2005, p. 602102, DOI: 10.1117/12.636491.
[31] I. S. Amiri, A. Afroozeh, and M. Bahadoran, "Simulation and analysis of multisoliton generation using a PANDA ring resonator system," *Chin. Phys. Lett.*, vol. 28, no. 10, p. 104 205, Oct. 2011.
[32] I. Amiri, J. Ali, and P. Yupapin, "Enhancement of FSR and finesse using add/drop filter and PANDA ring resonator systems," *Int. J. Modern Phys. B*, vol. 26, no. 4, pp. 1250034-1–1250034-13, Feb. 2012.
[33] X. Pang, X. Yu, Y. Zhao, L. Deng, D. Zibar, and I. T. Monroy, "Channel measurements for a optical fiber-wireless transmission system in the 75–110 GHz band," in *Proc. Asia-Pacific, MWP/APMP Microw. Photon. Int. Topical Meet. Microw. Photon. Conf.*, 2011, pp. 21–24.
[34] D. Duchesne, M. Ferrera, L. Razzari, R. Morandotti, B. Little, S. T. Chu, and D. J. Moss, "Nonlinear optics in doped silica glass integrated waveguide structures," in *Frontiers in Guided Wave Optics and Optoelectronics*, P. Bishnu, Ed. Rijeka, Croatia: InTech, 2010, pp. 269–294.
[35] S. Zlatanovic, J. S. Park, F. Gholami, J. Chavez Boggio, S. Moro, N. Alic, S. Mookherjea, and S. Radic, "Mid-infrared wavelength conversion in silicon waveguides pumped by silica-fiber-based source," *IEEE J. Sel. Topics Quantum Electron.*, vol. 18, no. 2, pp. 612–620, Mar./Apr. 2012.
[36] T. Inoue and S. Namiki, "Pulse compression techniques using highly nonlinear fibers," *Laser Photon. Rev.*, vol. 2, no. 1/2, pp. 83–99, Apr. 2008.
[37] A. Arbabi and L. L. Goddard, "Integrated optical resonators: Progress in 2011," *IEEE Photon. J.*, vol. 4, no. 2, pp. 574–577, Apr. 2012.
[38] H. Ma, Z. Chen, Z. Yang, X. Yu, and Z. Jin, "Polarization-induced noise in resonator fiber optic gyro," *Appl. Opt.*, vol. 51, no. 28, pp. 6708–6717, Oct. 2012.

[39] S. Songmuang, S. Punthawanunt, S. Mitatha, and P. Yupapin, "Photon switching using nonlinear PANDA ring resonator," *Proc. Eng.*, vol. 8, pp. 459–466, 2011.
[40] I. S. Amiri, A. Afroozeh, I. N. Nawi, M. A. Jalil, A. Mohamad, J. Ali, and P. P. Yupapin, "Dark soliton array for communication security," *Proc. Eng.*, vol. 8, pp. 417–422, 2011.
[41] I. S. Amiri, A. Afroozeh, J. Ali, and P. P. Yupapin, "Generation of quantum codes using up and down link optical soliton," *J. Teknol.*, vol. 55, no. S1, pp. 97–106, May 2012.
[42] I. Sadegh Amiri, M. Nikmaram, A. Shahidinejad, and J. Ali, "Generation of potential wells used for quantum codes transmission via a TDMA network communication system," *Sec. Commun. Netw.*, Feb. 14, 2013, to be published, DOI: 10.1002/sec.712.
[43] I. S. Amiri, M. H. Khanmirzaei, M. Kouhnavard, P. P. Yupapin, and J. Ali, "Quantum entanglement using multi dark soliton correlation for multivariable quantum router," in *Quantum Entanglement*, A. M. Moran, Ed. Commack, NY, USA: Nova, 2012.
[44] K. Uomwech, K. Sarapat, and P. Yupapin, "Dynamic modulated Gaussian pulse propagation within the double PANDA ring resonator system," *Microw. Opt. Technol. Lett.*, vol. 52, no. 8, pp. 1818–1821, Aug. 2010.
[45] I. S. Amiri and J. Ali, "Data signal processing via a Manchester coding–decoding method using chaotic signals generated by a PANDA ring resonator," *Chin. Opt. Lett.*, vol. 11, no. 4, p. 041901, Apr. 2013.
[46] I. S. Amiri, D. Gifany, and J. Ali, "Ultra-short multi soliton generation for application in long distance communication," *J. Basic Appl. Sci. Res.*, vol. 3, no. 3, pp. 442–451, Mar. 2013.
[47] X. An and R. Hekmat, "Directional MAC protocol for millimeter wave based wireless personal area networks," in *Proc. IEEE Veh. Technol. Conf. Spring*, 2008, pp. 1636–1640.
[48] A. Arvanitis, G. Anagnostou, N. Moraitis, and P. Constantinou, "Capacity study of a multiple element antenna configuration in an indoor wireless channel at 60 GHz," in *Proc. IEEE 65th Veh. Technol. Conf. Spring*, 2007, pp. 609–613.
[49] S. E. Gunnarsson, C. Karnfelt, H. Zirath, R. Kozhuharov, D. Kuylenstierna, A. Alping, and C. Fager, "Highly integrated 60 GHz transmitter and receiver MMICs in a GaAs pHEMT technology," *IEEE J. Solid-State Circuits*, vol. 40, no. 11, pp. 2174–2186, Nov. 2005.
[50] S. K. Yong, P. Xia, and A. Valdes-Garcia, *60 GHz Technology for Gbps WLAN and WPAN: From Theory to Practice*. Hoboken, NJ, USA: Wiley, 2011.